Journal of Chemical Technology and Metallurgy, 61, 5, 2026, 813-822

KINETIC MODELLING OF BORONIZING KINETICS OF THE SVERKER 3 STEEL WITH THE TAYLOR EXPANSION MODEL AND DIMENSIONAL ANALYSIS

Katia Benyakoub, Mourad Keddam, Brahim Boumaali

Laboratoire de Technologie des Matériaux
Faculté de Génie Mécanique et Génie des Procédés
USTHB, B.P. 32 El-Alia, 16111 Bab-Ezzouar
Algiers, Algeria, benyakoub.katia@gmail.com(K.B.); keddam@yahoo.fr (M.K.);
brahimboumaali@yahoo.com (B.B.).

Received 10 February 2026
Accepted 25 May 2026
DOI: 10.59957/jctm.v61.i5.2026.6

ABSTRACT

This study aims to model the boronizing kinetics of Sverker 3 steel in the temperature range 1173 - 1273 K for treatment times between 1 and 7 h. The first used approach is the Taylor expansion (TE) model. It considers the diffusion of boron atoms under transient regime through the surface of the treated Sverker 3 steel. Whereas the second one is the dimensional analysis (DA) model based on the Buckingham's Pi - theorem. It enables the reduction of the number of variables involved in complex physical phenomena. In formulating this second model, dimensionless groups were derived to simulate the thicknesses of the FeB and Fe_2B layers. The predicted values were found to be in good agreement with the experimentally measured layers' thicknesses. Furthermore, the boron activation energies determined for the FeB and Fe_2B layers were 214.92 kJ mol^{-1} and 203.20 kJ mol^{-1}, respectively, using Taylor Expansion (TE) model and were finally compared with values reported in the literature.

Keywords: *boride layers, boronizing, kinetics, activation energy, dimensional analysis model, Buckingham's Pi - theorem, Taylor expansion model.*

INTRODUCTION

Wear and corrosion are generally the most important mechanisms responsible for metal degradation, leading to component failure. Surface hardening of metals is one of the most widely used methods for enhancing surface properties. These engineered processes include chemical vapor deposition (CVD), physical vapor deposition (PVD), as well as thermochemical treatments such as carburizing, boriding, and nitriding. Particularly, boriding is a thermochemical treatment technique used for surface hardening of steels [1]. It involves the enrichment of the surface with boron atoms, which chemically react with iron atoms to form iron borides [1]. This process is carried out in a temperature range of 800 - 1050°C during 0.5 to 10 h using different methods and boron sources, it could be liquid boriding, plasma paste boriding, electrochemical boriding, solid boriding using paste or powder-pack boriding [2 - 6]. The resulting boride layers lead to an improvement in the surface properties of the treated material, such as high hardness and enhanced corrosion and wear resistance. Due to their low melting point, some metals cannot be used in boriding applications such as aluminum and magnesium [7]. From a practical point of view, the powder-pack boriding is the simplest among the available processes and requires low-investment equipment [8]. As previously mentioned, the steels are widely used in boriding, therefore, two types of boride layers (FeB and Fe_2B) can be formed over the steel's surface. The Fe_2B layer is under compressive stress, with hardness values ranging from 1400 to 1750HV, whereas the FeB layer is under tensile stress and exhibits higher hardness values, between 2000 and 2300 HV [9]. Therefore, the propagation of cracks can occur across the (FeB / Fe_2B) interface [7]. For this reason, the Fe_2B layer is preferred over the bilayer (FeB + Fe_2B) for industrial applications, that require resistance to mechanical fatigue [10, 11]. To optimize the thickness of boride layers according to the working conditions of borided steels, different kinetic approaches have been suggested in the literature [12 - 18]. For example, Ortiz-Dominguez et al. used two different approaches to model the growth kinetics of Fe_2B layer on AISI 1018 steel [12]. The first method was based on the mass balance equation at the Fe_2B / substrate interface, while the second involved the formulation of an equation using dimensional analysis to describe the layer thickness as a function of the processing parameters (temperature and time). Finally, their experimentally measured layers' thicknesses were compared with the predicted values, showing good agreement. Keddam and Kulka applied the Dybkov model and the average diffusion coefficient model to simulate the kinetics of FeB and Fe_2B layers on AISI D2 steel, using three different durations (2, 4 and 6 h) and a temperature range 1223 - 1273K [13].

They observed that the experimental layer thicknesses were consistent with the predicted values. In a subsequent study, Keddam et al. implemented the Taylor expansion (TE) based model to simulate boron diffusion in AISI 316L steel [14]. This method employs a second order Taylor expansion to describe the boron concentration profile under transient diffusion conditions. The activation energies of boron diffusion in the FeB and Fe_2B phases for AISI 316L steel were also calculated using the experimental data from the literature. To confirm the validity of the model the authors used two processing conditions, 1173K for 0.75 h and 1223K for 1.75 h, the results showed good agreement between simulated and experimental results. In another research paper, Benyakoub et al. [11] applied the linear mass balance equations-based model and the dimensional analysis using the experimental data about the boriding kinetics of 4Cr5MoSiV1 steel [15]. They obtained a good agreement between the predicted values from both approaches and the experimentally measured thicknesses. Consequently, the activation energies derived from the bilayer model were 164.92 $kJ.mol^{-1}$ for FeB and 153.39 $kJ.mol^{-1}$ for Fe_2B. Campos et al. [16] and Torres et al. [17] derived dimensional analysis - based relations for borided AISI M2 and AISI 1045 steels using the paste boriding technique. For each boride layer, they identified two dimensionless groups that were linked through a power - law relationship, which was then fitted to predict the layers' thicknesses. Benyakoub et al. simulated the boriding kinetics of Sverker 3 steel using mass balance equations under a steady diffusion regime for the FeB and Fe_2B layers [18]. They introduced two dimensionless constants, and the model was experimentally validated under three different processing conditions: 975°C for 10 h, and 1050°C for 5 h and 7 h. Ptačinová et al., in their study, employed the average diffusion coefficient model, assuming that the boron concentration profiles along the boronized layers were linear [19]. The resulting boron activation energies were 215.18 kJ mol^{-1} for FeB and 203.6 $kJ.mol^{-1}$ for Fe_2B, which are highly comparable to those reported by Benyakoub et al. [18].

In this study, two approaches were employed to simulate the growth kinetics of the FeB and Fe_2B layers on Sverker 3 steel using experimental data from Benyakoub at al. [18] and Ptačinová et al. [19]. The first one is the Taylor expansion model [14]. This approach utilizes a second-order Taylor expansion of boron distribution across each formed boride layer. The solutions for the resulting differential equations were derived by approximating the temperature change in the boron diffusivities in iron borides FeB and Fe_2B, using Arrhenius relations. The second one based on the Buckingham's Pi - theorem, for each layer, two dimensionless groups were derived, and fitting the kinetic data to power-law relationships allowed the determination of the constants involved. Additionally, the boron activation energies for FeB and Fe_2B were calculated and compared with values reported in the literature. Finally, the two used approaches have been validated using three different boriding conditions for the boriding kinetics of Sverker 3 steel.

EXPERIMENTAL

The Taylor expansion (TE) model was applied to simulate the boriding kinetics of Sverker 3 steel using analytical solutions of derived set of two differential equations of first order [14]. Fig. 1. gives the evolution of developed boron concentration profiles across the bilayer (FeB / Fe_2B). The boride incubation times for FeB and (FeB + Fe_2B) layers were ignored during the application of this kinetic model. The upper and lower boron contents in FeB are C_{up}^{FeB} (= 16.40 wt. %B) and C_{low}^{FeB} (= 16.23 wt. %B), respectively. For the Fe_2B phase the corresponding concentrations values are $C_{up}^{Fe_2B}$ (= 9 wt. %B) and $C_{low}^{Fe_2B}$ (= 8.83 wt. %B), respectively [20]. C_{ads} represents the boron amount being adsorbed at the steel surface [21]. The variable u is FeB layer thickness

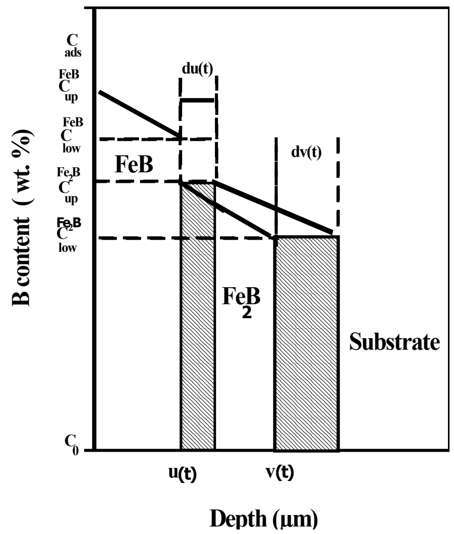

Fig.1. Schematic representation of boron concentration profiles across the bilayer.

and ν that of the bilayer (FeB / Fe_2B). C_o represents the maximal solubility of boron atoms in the matrix whose value is 35 × 10^{-4} wt. % B [22]. Eq. (1) gives the expression of FeB layer thickness.

$$u(t) = k'\sqrt{t} = 2\varepsilon_1\sqrt{D_{FeB}t} \qquad (1)$$

The parameter k′ is the kinetic constant for the FeB phase, ε_1 is a dimensionless constant and D_{FeB} the boron diffusion coefficient in FeB. Eq. (2) gives the expression of the bilayer (FeB / Fe_2B) thickness:

$$v(t) = k\sqrt{t} = 2\varepsilon_2\sqrt{D_{Fe_2B}t} \qquad (2)$$

The parameter k represents the parabolic growth constant at the (FeB / Fe_2B) interface, ε_2 is a dimensionless constant and D_{Fe2B} the B diffusion coefficient in Fe_2B. The (TE) model is therefore based upon solving the set differential equations given by Eqs. (3) and (4):

$$\frac{u}{D_{FeB}}\left\{w_1(\frac{du}{dt})+[1+\frac{(v-u)}{D_{Fe_2B}}(\frac{dv}{dt})](w_2\frac{dv}{dt}+w_{12}\frac{du}{dt})\right\}[1+$$
$$+\frac{u}{2D_{FeB}}(\frac{du}{dt})] = (C_{up}^{FeB}-C_{low}^{FeB}) \qquad (3)$$

$$\frac{(v-u)}{D_{Fe_2B}}\left\{w_2\frac{dv}{dt}+w_{12}\frac{du}{dt}\right\}[1+\frac{(v-u)}{2D_{Fe_2B}}(\frac{dv}{dt})] =$$
$$= (C_{up}^{Fe_2B}-C_{low}^{Fe_2B}) \qquad (4)$$

Eqs. (5) and (6) give the exact analytical solutions for the two dimensionless parameters ε_1 and ε_2:

$$\varepsilon_1 = \sqrt{\frac{1}{2}[-1+\sqrt{1+\frac{4k'w_{11}}{(w_1k'+\sqrt{(w_2k+w_{12}k')^2+4kw_{12}(w_2k+w_{12}k')})}}]} \qquad (5)$$

$$\varepsilon_2 = \sqrt{\frac{k}{2(k-k')}[-1+\sqrt{1+\frac{4kw_{12}}{(w_2k+w_{12}k')}}]} \qquad (6)$$

with $w_1 = [\frac{(C_{up}^{FeB}+C_{low}^{FeB})}{2} - C_{int}^{Fe_2B})]$

and $w_2 = [\frac{(C_{int}^{Fe_2B}+C_{low}^{Fe_2B})}{2} - C_0)]$, $w_{11} = \frac{(C_{up}^{FeB}-C_{low}^{FeB})}{2}$, and $w_{12} = \frac{(C_{up}^{Fe_2B}-C_{low}^{Fe_2B})}{2}$

Determining the numerical values of these two dimensionless parameters, the boron diffusion coefficients in each phase (FeB or Fe_2B) can be estimated from Eqs. (7) and (8):

$$D_{Fe_2B} = (\frac{k}{2\varepsilon_2})^2 \qquad (7)$$

$$D_{FeB} = (\frac{k'}{2\varepsilon_1})^2 \qquad (8)$$

The dimensional analysis is a useful and powerful tool helping to find or check relations between physical quantities and ensure the consistency of units in any physical equation by reducing the number of variables in the physical problem. It can also give global laws for all cases [23, 24]. A dimension of a physical quantity is defined as a combination of different dimensions describing this quantity. The most common basic dimensions are the mass [M], the time [T], length [L]. As an example, the velocity ν has the dimension [LT^{-1}] but can be expressed by different units as m s^{-1} or km h^{-1}. Considering the newton's second law f = ma, the force unit is expressed by Newton, but the dimension can be expressed with the dimension of the second term of the equation [F] = [m] [a] which is [F] = [M] [LT^{-1}], therefore, the dimension of [F] = [M LT^{-1}]. So, the establishment of the dimensionless parameters can be physically meaningful. As per the Buckingham's Pi - theorem, every physical equation containing n variables can be written as an equation of (n - m) dimensionless parameters where m is the number of the physical independent quantities expressing the *n* variables [23].

In this study, the dimensional analysis based on the Buckingham's Pi - theorem is used to analyse the time dependencies of the boride layers' thicknesses of the

Sverker 3 steel. This theorem is based on the creation of dimensionless groups $\Pi_{(n-m)}$. These products are dimensionless and represent the most parameters of the system. To reduce the complexity of the problem, every Π_i dimensionless group can be written as a function of others using the products of power laws. Moreover, fitting the experimental data with a power law is a common approach to describe the classical parabolic behaviour where the exponent is deducted close to 0.5, this fitting was observed in the case of borided steels [25, 26]. For the boriding treatment, five variables can be found for each boride layer u and l, where *u*, l = (ν - u) and ν are the thicknesses of FeB and Fe_2B layers and those of the bilayer (FeB + Fe_2B), respectively. These variables are as follows: $u = u(t, \lambda_{\max}, C_{FeB}, k')$ and $l = l(t, \lambda_{\max}, C_{Fe_2B}, k_1)$ where t is the time duration of the process, C_{FeB} and C_{Fe_2B} are the boron concentrations in the FeB and Fe_2B layers respectively, k' and $k_1 = (k - k')$ are the parabolic constants of the FeB and Fe_2B layers respectively. *k* stands for the parabolic growth constant at the (FeB / substrate) interface. $\lambda_{\max}$ is the maximum depth of boron atoms diffusion from the surface into the substrate (iron phase), corresponding to the highest temperature and longest time duration [11]. Its expression is given by Eq. (9):

$$\lambda_{\max} = \sqrt{t_{\max} D(T_{\max})} \quad (9)$$

Where $D(T_{\max})$ is the B diffusion coefficient in the iron phase, given in $m^2\ s^{-1}$, for the highest temperature of the process and expressed with Eq. (10) [27]:

$$D = 4.4 \times 10^{-8} \exp\left(-\frac{81.5\ kJ\ mol^{-1}}{RT}\right) \quad (10)$$

where T is the temperature expressed in Kelvin and $R = 8.314\ J\ mol^{-1}\ K^{-1}$ is the ideal gas constant. The experimental parabolic growth constants k' and k obey the Arrhenius relationship, and their expressions can be written as in Eq. (11) and Eq. (12):

$$k' = \exp\left(\frac{a_{11}}{T} + b_{11}\right) \quad (11)$$

$$k = \exp\left(\frac{a_{22}}{T} + b_{22}\right) \quad (12)$$

By applying the Buckingham's Pi - theorem, two dimensionless groups can be formed for each layer. Based on the three common dimensions M, L, T and for the FeB layer each group can be written as:

$$\Pi_{u_1} = u \lambda_{\max}^{a_1} k'^{a_2} C_{FeB}^{a_3} \quad (13)$$

$$\Pi_{u_2} = t \lambda_{\max}^{b_1} k'^{b_2} C_{FeB}^{b_3} \quad (14)$$

By applying the dimensional analysis principle, Eq. (15) and Eq. (16) can be obtained as follows:

$$\Pi_{u_1} = \frac{u}{\lambda_{\max}} \quad (15)$$

$$\Pi_{u_2} = t\left(\frac{k'}{\lambda_{\max}}\right)^2 \quad (16)$$

The same mathematical operation applies to the Fe_2B layer, and the obtained dimensionless groups can be expressed by Eqs. (17) and (18):

$$\Pi_{u_1} = u \lambda_{\max}^{a_1} k'^{a_2} C_{FeB}^{a_3} \quad (17)$$

$$\Pi_{u_2} = t \lambda_{\max}^{b_1} k'^{b_2} C_{FeB}^{b_3} \quad (18)$$

And by using the dimensional analysis principle, Eq. (19) and Eq. (20) can be derived as:

$$\Pi_{l_1} = \frac{l}{\lambda_{\max}} \quad (19)$$

$$\Pi_{l_2} = t\left(\frac{k_1}{\lambda_{\max}}\right)^2 \quad (20)$$

Hence, the thicknesses of the FeB and Fe_2B layers can be predicted from the experimental data using power-law fitting, as expressed in Eq. (21) and Eq. (22):

$$\Pi_{u_1} = \alpha_1 (\Pi_{u_2})^{\beta_1} \quad (21)$$

$$\Pi_{l_1} = \alpha_2 (\Pi_{l_2})^{\beta_2} \quad (22)$$

As a result, the expressions of the simulated layers' thicknesses of the FeB and (Fe_2B) layers are respectively given by Eq. (23) and Eq. (24):

$$u = \frac{\alpha_1 t^{\beta_1}}{\lambda_{\max}^{(2\beta_1 - 1)}} \left(\exp\left(\frac{a_{11}}{T} + b_{11}\right)\right)^{2\beta_1} \quad (23)$$

$$v = u + \frac{\alpha_2 t^{\beta_2}}{\lambda_{\max}^{(2\beta_2 - 1)}} \left(\exp\left(\frac{a_{22}}{T} + b_{22}\right) - \exp\left(\frac{a_{11}}{T} + b_{11}\right)\right)^{2\beta_2} \quad (24)$$

RESULTS AND DISCUSSION

To validate the presented models, the experimental data from Benyakoub et al. [18] and Ptačinová et al.

Table 1. Chemical composition (in weight %) of Sverker 3 steel.

Element	C	Cr	W	Mn	Si	Fe
wt.%	2.05	12.7	1.1	0.8	0.3	Balance

Table 2. Kinetic constants values of the two growth fronts in the range of 1173 - 1273K [18, 19].

T (K)	1173	1223	1248	1273
k' (µm s$^{-0.5}$)	0.1618	0.2563	0.3172	0.3905
k (µm s$^{-0.5}$)	0.3339	0.5215	0.6399	0.7703

were employed for this purpose [19]. Table 1 gives the chemical composition of Sverker 3 steel used as substrate for the powder - pack boriding process. The samples were cut from a wrought bar and grinded until obtaining a fine surface. After that, they were cleaned, dried and placed in stainless steel containers and then embedded in a Durborid powder mixture. The powder - pack boronizing process was carried out between 1173 and 1273K for 1, 3, 5 and 7 h. After the treatment, the containers were taken out of the furnace and were let to cool at the ambient temperature. Afterwards, they were cleaned, cross-sectioned and etched with Nital solution (3 vol. %) to reveal their microstructures. The microstructural analysis of the treated samples showed the presence of both layers (FeB and Fe_2B) for almost processing parameters and their crystalline nature were confirmed by the XRD analysis. A flat morphology of phase interfaces was obtained in this case due to the influence of the alloying elements present in the Sverker 3 steel and other alloy steels [28, 29]. The obtained layers' thicknesses were measured using SEM micrographs according to the practical procedure developed by Kunst and Schaaber [30]. A total of thirty measurements were done on the cross - sections of treated steels to obtain reliable averaged values of layers' thicknesses. The experimental data reported by Benyakoub et al. [18] and Ptačinová et al. [19] were used to apply the dimensional analysis approach for predicting the thicknesses of the boride layers. This approach made it possible to establish curves relating the layer thicknesses to the square root of time. It should be noted that at 900°C and after 1 h of thermochemical treatment, the Fe_2B layer was very thin, whereas the FeB layer was not formed at all. Subsequently, the kinetic constants k' and k, corresponding to the two growth fronts within the temperature range 1173 - 1273 K, were inferred from the slopes of the plotted straight lines and are summarized in Table 2.

According to the Eq. (11) and Eq. (12) and after linear fitting with the Arrhenius relationships, the temperature-dependent expressions of k' and k expressed in m s$^{-0.5}$, are given by Eq. (25) and Eq. (26):

$$k' = \exp(\frac{-13150}{T} - 4.426) \tag{25}$$

$$k = \exp(\frac{-12525}{T} - 4.2307) \tag{26}$$

The numerical values of dimensionless constants ε_1 and ε_2 were determined by using the data presented in Table 2 for different temperatures. The results showed that these calculated values remain nearly invariant ($\varepsilon_1 = 0.0573$ and $\varepsilon_2 = 0.1364$) while changing the processing temperatures, as summarized in Table 3. This result confirms that the growth kinetics of the boronized layers follows a parabolic law. Furthermore, the data in Table 3 were fitted using the Arrhenius relationship, to determine the boron diffusion coefficients in FeB and Fe_2B by plotting the corresponding straight lines shown in Fig. 2. Their expressions given by Eqs. (27) and (28) were then deduced.

$$D_{FeB} = 7.54 \times 10^{-3} \exp(-\frac{214.92\ kJ\ mol^{-1}}{RT}) \tag{27}$$

$$D_{Fe_2B} = 1.73 \times 10^{-3} \exp(-\frac{203.20\ kJ\ mol^{-1}}{RT}) \tag{28}$$

Afterwards, the boron activation energies values for FeB and Fe_2B were deduced as equal to 214.92 kJ.mol^{-1} and 203.20 kJ.mol^{-1}, respectively. Table 4 compares the obtained boron activation energies in FeB and Fe_2B for Sverker 3 steel with the literature results [3, 18 - 20, 31 - 36]. As seen in Table 4, the reported boron activation energies for different steels vary. This difference in the values can be attributed to several factors, including the choice of processing parameters, the

Table 3. Values of boron diffusion coefficients in FeB and Fe_2B layers for the Sverker 3 steel calculated with the Taylor Expansion (TE) model.

T, K	1173	1223	1248	1273
$D_{FeB} \times 10^{-12}$ ($m^2 s^{-1}$)	2.02	5.02	7.64	11.39
$D_{FeB} \times 10^{-12}$ ($m^2 s^{-1}$)	1.52	3.67	5.48	7.77
ε_1	0.0569	0.0572	0.0573	0.0578
ε_2	0.1351	0.1360	0.1366	0.1381

Table 4. Comparison of obtained boron activation energies in FeB and Fe_2B for the Sverker 3 steel with the literature results.

Steel	Boriding type	Temperature range, K	Activation energy, kJ mol^{-1}	Calculation method	Refs.
AISI 8620	Plasma paste	973 - 1073	99.77-108.24 (FeB + Fe_2B)	Parabolic growth law	[3]
AISI D2	Salt bath	1073 - 1273	170 (FeB + Fe_2B)	Parabolic growth law	[31]
AISI 1018	Pulsed DC powder	973 - 1123	133.8 - 152.3 (FeB) 129.5 - 145.9 (Fe_2B)	Dybkov model	[32]
AISI 316L	Pulsed DC powder	1123 - 1273	157 ± 4.5 (FeB) 148.7 ± 2.1(Fe_2B)	Integral method	[33]
AISI W1	Powder	1123 - 1323	171.2 ± 16.6 (FeB + Fe_2B)	Parabolic growth law	[34]
Nitronic - 50	Powder	1198 - 1248	186.5 (FeB + Fe_2B)	Parabolic growth law	[35]
34CrAlNi7	Powder	1123 - 1323	169.40 (FeB) 165.27 (Fe_2B)	Integral method	[20]
AISI M2	Powder	1173 - 1323	223 (FeB) 209 (Fe_2B)	Diffusion model	[36]
Sverker 3	Powder	1173 - 1273	215.20 (FeB) 202.95 (Fe_2B)	Bilayer Model	[18]
Sverker 3	Powder	1173 - 1273	215.18 (FeB) 203.61 (Fe_2B)	ADC model	[19]
Sverker 3	Powder	1173 - 1273	214.92 (FeB) 203.20 (Fe_2B)	(TE) model	This work

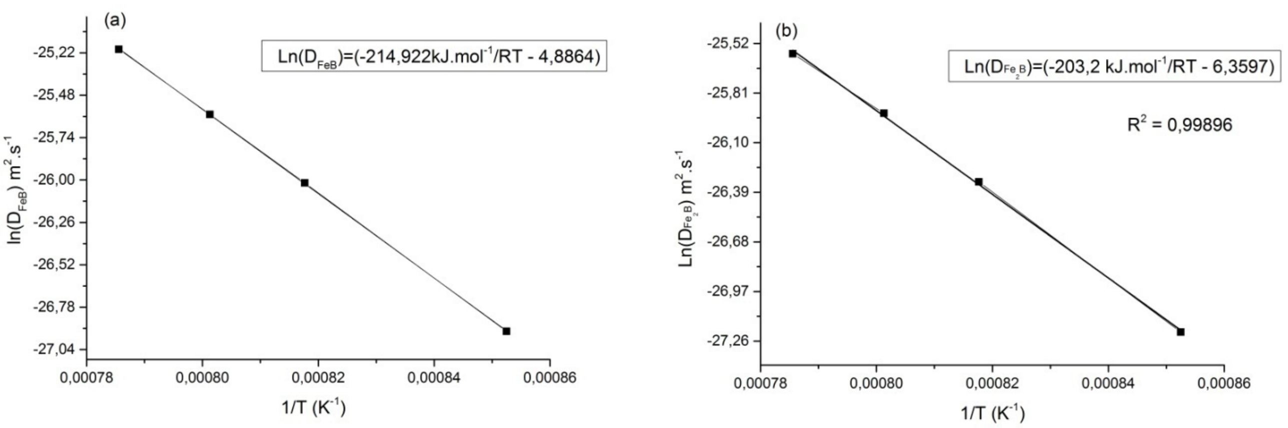

Fig. 2. Arrhenius Fitting of the boron diffusion coefficients as a function of the inverse of temperature: (a) FeB; (b) Fe_2B.

boriding method, and the chemical composition of the steels. The calculated values of boron activation energies also depend on the method used, such as the classical parabolic growth law [3, 31, 35] or other kinetic approaches [18 - 20, 32, 33, 36]. It is worth noting that the obtained boron activation energies are in line with those reported for the same steel by Benyakoub at al. [18] and Ptačinová et al. [19].

To experimentally validate the dimensional analysis model, a nonlinear regression was performed on the dimensionless groups using a power-law fit. The results of this fitting are summarized in Table 5. The evolution of the respective dimensionless groups for FeB and Fe_2B, is shown in the Fig. 3. To plot these two curves, the numerical value of maximum boron penetration in the substrate is then required. Its value was 708 µm at 1273K for 7 h, using the value of diffusion coefficient in the g - Fe phase [27] determined at this temperature. The arithmetic mean values of a_1 ,a_2 ,b_1, b_2 were respectively 1.0042 ,1.0355 ,0.5006 and 0.5017. Therefore, the parabolic regime of the growth kinetics of FeB and Fe_2B was established by these values, since they are nearly identical to the values observed in the basic parabolic law which are 1 for a and 0.5 for b. The time - dependent thicknesses of the simulated layers, predicted by the dimensional analysis model, are compared with the experimental thicknesses in Fig. 4. This comparison demonstrates a good fit with the experimental data. Additionally, the kinetic data obtained at 900°C for 1 h regarding the FeB layer thickness was not considered, as the FeB layer did not form. Some slight inconsistencies can also be observed in the plots between the calculations and the experiments, due to the use of arithmetic mean values for the fitting coefficients. To validate the Taylor expansion model, three additional boriding conditions were considered corresponding to the processing parameters (1248 K for 10 h, 1323 K for 5 h and 1323 K for 7 h). The experimental layers' thicknesses were then compared with those from the Taylor expansion model and the dimensional analysis model. In Table 6 are grouped the thicknesses of layers u

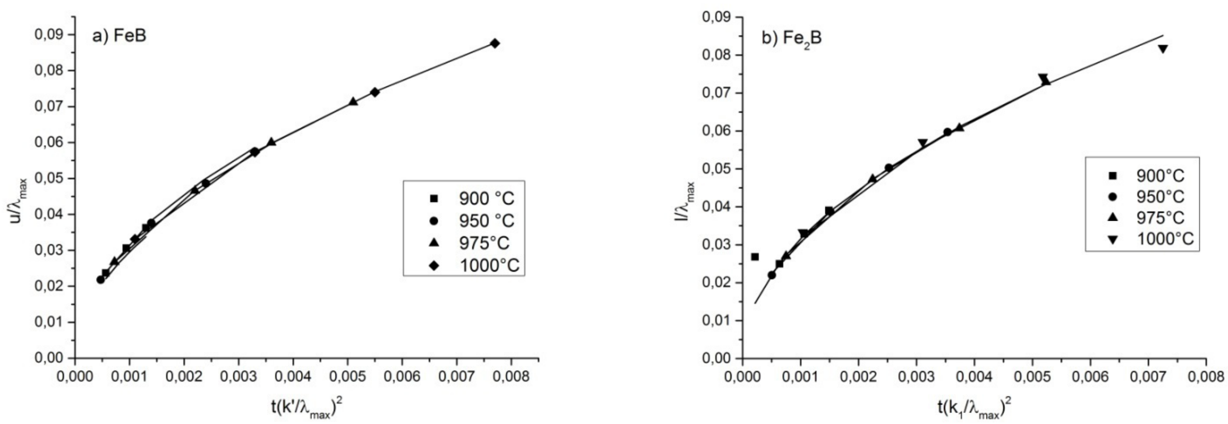

Fig. 3. Evolution of the formed dimensionless groups for: (a) FeB; (b) Fe_2B.

Table 5. Determined constants from the power-law fitting of the experimental data: a) for FeB; b) for Fe_2B.

a) For FeB:				
T(K)	1173	1223	1248	1273
a_1	1.011	0.9958	1.008	1.002
b_1	0.5017	0.4992	0.5015	0.5003
b) For Fe_2B:				
T(K)	1173	1223	1248	1273
a_2	1.208	1.079	1.057	0.7982
b_2	0.5268	0.5127	0.5098	0.4576

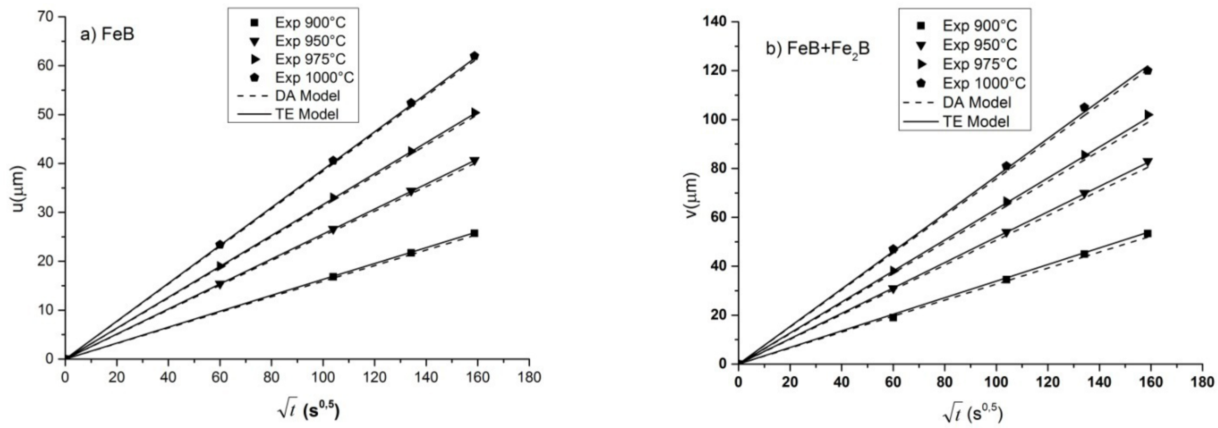

Fig. 4. Evolution of the simulated layers' thicknesses as a function of the square root of time: (a) FeB; (b) FeB + Fe_2B. The symbols are the experimental points [18, 19].

Table 6. Confrontation of the experimental layers' thicknesses [18] with the simulated thicknesses using the Taylor expansion and dimensional analysis models.

Processing Parameters	u_{exp}, µm [18]	u_{sim}, µm (TE) model	u_{sim}, µm (DA) model	v_{exp}, µm [18]	v_{sim}, µm (TE) model	v_{sim}, µm (DA) model
975°C for 10 h	65 ± 2.1	59.88	60.31	124 ± 2	119.35	122.53
1050°C for 5 h	74 ± 3	76.18	77.52	154 ± 4	147.03	153.06
1050°C for 7 h	87 ± 3	90.13	91.74	172 ± 4	173.97	181.17

and v, predicted by both approaches and compared with experimental thicknesses [18]. The numerical value of λ_{max} together with the arithmetic values of the constants involved in both models, are needed to do these calculations. Despite some simplifying assumptions, the results presented in Table 6 are consistent with the experimental layers' thicknesses for three different boriding conditions. Overall, the used approaches demonstrate their capability to successfully simulate the boriding kinetics of Sverker 3 steel. The dimensional analysis (DA) model using the Buckingham's Pi - theorem provided the key advantage of a simple mathematical formulation, allowing for the simulation of layers' thicknesses for the selected boriding conditions. It can also be applied to other thermochemical treatments such as nitriding and carburizing. For the case of Sverker 3 steel, the results indicated a likely formation of CrB metal borides as precipitates, which hindered boron diffusion to greater depths and were not accounted for when formulating this dimensional analysis model. The comparison of the calculated results with the experimental data confirmed the capability of the utilized models to simulate the diffusion kinetics of boron in Sverker 3 steel.

CONCLUSIONS

This work is concerned with the kinetic analysis of FeB and Fe_2B layers on Sverker 3 steel using two distinct approaches, the Taylor expansion (TE) and the dimensional analysis (DA) models. The first model enabled exact solutions to be derived from the two differential equations governing the growth kinetics of the boride layers. The boron activation energies were determined as 214.92 kJ.mol^{-1}for FeB and 203.20 kJ mol^{-1}for Fe_2B in the Sverker 3 steel. The application of the Buckingham's Pi - theorem simplified the problem by establishing two key dimensionless groups, which were related through a power law, thereby corroborating the nature of growth law of boride layers. The dimensional analysis model provided simple expressions for the thicknesses of the FeB and (FeB + Fe_2B) layers. Both models were then successfully validated using three boriding conditions and a good agreement was achieved between the simulated layers' thicknesses and those obtained experimentally. As a prospect, both models can be applied to other alloys to simulate the kinetics diffusion of elements for other thermochemical treatments.

Acknowledgments

No external funding was provided for this research. The study was conducted as part of the PRFU project, registered under the reference number A11N01UN160420230012. The project received support from the Ministry of Higher Education and Scientific Research of Algeria and was coordinated by the (DGRSDT, Algeria).

Authors' contributions

Conceptualization, K.B. and M.K. (Mourad Keddam); data curation, K.B., M.K. and B.B.; formal analysis, K.B. and M.K.; funding acquisition, M.K.; investigation, K.B., M.K. and BB.; methodology, K.B., M.K., and B.B.; project administration, M.K.; resources, K.B. and M.K.; supervision, K.B. and M.K.; validation, K.B. and M.K.; visualization, K.B., M.K., and B.B. writing-original draft, K.B. and M.K.; writing-review and editing, K.B. and M.K. All authors have read and agreed to the published version of the manuscript.

REFERENCES

1. M. Kułka, Current trends in boriding: Techniques and applications, Springer International Publishing, 2019.
2. M.A. Khater, S.A. Bouaziz, M.A. Garrido, P. Poza, Mechanical and tribological behaviour of titanium boride coatings processed by thermochemical treatments, Surf. Eng., 37, 1, 2021, 101-110.
3. I. Gunes, S. Ulker, S. Taktak, Kinetics of plasma paste boronized AISI 8620 steel in borax paste mixtures., Prot. Met. Phys. Chem. Surf., 49, 2013, 567-573.
4. A. Kaouka, K. Benarous, Electrochemical boriding of titanium alloy Ti - 6Al - 4V, J. Mater. Res. Technol., 8, 6, 2019, 6407-6412.
5. D.M. Flores - Arcos, N. López - Perrusquia, M.A. Doñu - Ruiz, M. Flores - Martínez, S. Muhl-Saunders, D.S. Huitron, E.D. García-Bustos, The effects of the finishing polish process on the tribological properties of boride surfaces of AISI 4140 steel, Coatings, 15, 4, 2025, 474.
6. H.O. Tan, S. Atasoy, S. Aktaş, The effect of boriding temperature and time on the structural and mechanical properties of M42 steel, Turk. Doga Ve Fen Derg., 13, 2, 2024, 1-5.
7. M. Ortiz - Domínguez, Á.J. Morales - Robles, O.A. Gómez - Vargas, G. Moreno - González, Surface growth of boronized coatings studied with mathematical models of diffusion, Metals, 14, 6, 2024, 670.
8. V. Jain, G. Sundararajan, Influence of the pack thickness of the boronizing mixture on the boriding of steel, Surf. Coat. Technol., 149, 2002, 21-26.
9. Z. Pala, J. Fojtikova, T. Koubsky, R. Musalek, J. Strasky, J. Capek, J. Kyncl, L. Beranek, K. Kolarik, Study of residual stresses, microstructure, and hardness in FeB and Fe_2B ultra-hard layers, Powder Diffraction., 30, S1, 2015, S83-S89.
10. A. Barkat, H. Djilali, O. Allaoui, Effect of boriding on the fatigue resistance of C20 carbon steel, Acta Phys. Pol. A, 132, 3, 2017, 813-816.
11. K. Benyakoub, M. Keddam, B. Boumaali, M. Kulka, Kinetic modelling of powder-pack boronized 4Cr-5MoSiV1 steel by two distinct approaches, Coatings, 13, 6, 2023, 1132.
12. M. Ortiz - Domínguez, I. Campos - Silva, E. Hernández - Sánchez, J. Nava - Sánchez, J. Martínez - Trinidad, M.Y. Jiménez - Reyes, O. Damián - Mejía, Estimation of Fe_2B growth on low-carbon steel based on two diffusion models, Int. J. Mater. Res., 102, 4, 2011, 429-434.
13. M. Keddam, M. Kulka, Simulation of boriding kinetics of AISI D2 steel using two different approaches, Met. Sci. Heat Treat., 61, 11 - 12, 2020, 756-763.
14. M. Keddam, Z. Nait Abdellah, P. Jurči, Modelling the boron diffusion in AISI 316 L steel with the Taylor expansion approach, Metall. Res. Technol.,123, 3, 2026, 306.
15. O. Delai, C. Xia, L. Shiqiang, Growth kinetics of the FeB / Fe_2B boride layer on the sur-face of 4Cr5MoSiV1 steel: Experiments and modelling, J. Mater. Res. Technol., 11, 2021, 1272-1280.
16. I. Campos, R. Torres, Growth kinetics of iron boride layers: Dimensional analysis, Appl. Surf. Sci., 252, 24, 2006, 8662-8667.
17. R. Torres, I. Campos, G. Ramírez Sandoval, O. Bautista, J. Martinez, Dimensional anal-ysis in the growth kinetics of FeB and Fe_2B layers during the boriding process, Int. J. Micro-struct. Mater. Prop.,

2, 2, 2007, 203-215.
18. K. Benyakoub, M. Keddam, J. Ptačinová, Z. Gabalcová, B. Boumaali, P. Jurči, Boride layers on Sverker 3 steel: Kinetic modeling, experimental characterization, and validation, Prot. Met. Phys. Chem. Surf., 59, 6, 2023, 1250-1259.
19. J. Ptačinová, Z. Gabalcová, J. Ďurica, M. Drienovský, M. Keddam, P. Jurči, Characterization of dual phase boride coatings on Sverker 3 steel and simulation of boron diffusion, Mater. Test., 65, 4, 2023, 578-592.
20. M. Keddam, P. Topuz, A kinetic approach for assessing boron diffusivities in iron boride layers formed on 34CrAlNi7 steel, J. Chem. Technol. Metall., 57, 4, 2022, 824-833.
21. L.G. Yu, X.J. Chen, K.A. Khor, G. Sundararajan, FeB/Fe2B phase transformation during SPS pack - boriding: Boride layer growth kinetics, Acta Mater., 53, 8, 2005, 2361-2368.
22. H. Okamoto, B - Fe (Boron - Iron), J. Phase Equilibria Diff., 25, 2004, 297-298.
23. B. Zohuri, Dimensional analysis beyond the Pi theorem, Springer International Publish-ing, 2017.
24. W. Chen, Dimensional analysis and complex analysis: An analogy via singularity types, Center for Open Science, 2025.
25. I. Campos, J. Oseguera, U. Figueroa, J.A. García, O. Bautista, G. Kelemenis, Kinetic study of boron diffusion in the paste-boriding process, Mater. Sci. Eng. A, 352, 1-2, 2003, 261-265.
26. S. Sen, U. Sen, C. Bindal, The growth kinetics of borides formed on boronized AISI 4140 steel, Vacuum, 77, 2, 2006, 195-202.
27. P. Guiraldenq, Diffusion dans les métaux, Techniques de l'Ingénieur, MB1 (M 55),1978.
28. A. García - León, J. Martínez - Trinidad, I. Campos-Silva, W. Wong - Angel, Mechanical characterization of the AISI 316L alloy exposed to boriding process, DYNA, 87, 213, 2020, 34-41.
29. S. Taktak, S. Tasgetiren, Identification of delamination failure of boride layer on com-mon Cr-based steels, J. Mater. Eng. Perform., 15, 2006, 570-574.
30. H. Kunst, O. Schaaber, Beobachtungen beim oberflaechenborieren von Stahl, HTM Haerterei Techn. Mitt., 22, 1, 1967, 1-25.
31. S. Sen, U. Sen, and C. Bindal, An approach to kinetic study of borided steels, Surf. Coat. Technol., 191, 2, 2005, 274-285.
32. K.D. Chaparro - Perez, M. Olivares-Luna, J.L. Rosales - Lopez, L.E. Castillo - Vela, F.P. Espino-Cortes, L.M. Hernandez-Simon, I. Campos - Silva, Insights on the pulsed - DC powder - pack boriding process: Kinetic, statistic, and electric field dynamics in low and medium temperatures, Surf. Coat. Technol., 494, 2024, 131390.
33. I. Campos-Silva, J. Cedeño - Velázquez, A.D. Contla - Pacheco et al., Microstructural and kinetics analysis of FeB - Fe_2B layer grown by Pulsed-DC powder-pack boriding on AISI 316 L steel, J. Vac. Sci. Technol. A 42, 2024, 053101.
34. C. Bindal, Kinetics of boriding of AISI W1 steel, Mater. Sci. Eng. A., 347, 1 - 2, 2003,311-314.
35. R. Hariharan, R. Balasundaram, K. Lenin, D.J. Jefrey, Enhancing the surface character-istics of Nitronic-50 through pack boronizing, Chem. Pap., 79, 2025, 4303-4316.
36. I. Campos - Silva, M. Ortiz - Dominguez, C. Tapia-Quintero, G. Rodríguez - Castro, M.Y. Jiménez - Reyes, E. Chávez - Gutiérrez, Kinetics and Boron Diffusion in the FeB / Fe_2B layers Formed at the Surface of Borided High - Alloy Steel, J. Mater. Eng. Perform., 21, 2012, 1714-1723.